JACS
JOURNAL OF THE AMERICAN CHEMICAL SOCIETY

COMMUNICATION

pubs.acs.org/JACS

HNO Binding in a Heme Protein: Structures, Spectroscopic Properties, and Stabilities

Liu Yang,[†] Yan Ling,[‡] and Yong Zhang*[,†,‡]

[†]Department of Chemistry, Chemical Biology, and Biomedical Engineering, Stevens Institute of Technology, Castle Point on Hudson, Hoboken, New Jersey 07030, United States

[‡]Departments of Chemistry and Biochemistry, University of Southern Mississippi, 118 College Drive #5043, Hattiesburg, Mississippi 39406, United States

Supporting Information

ABSTRACT: HNO can interact with numerous heme proteins, but atomic level structures are largely unknown. In this work, various structural models for the first stable HNO heme protein complex, MbHNO (Mb, myoglobin), were examined by quantum chemical calculations. This investigation led to the discovery of two novel structural models that can excellently reproduce numerous experimental spectroscopic properties. They are also the first atomic level structures that can account for the experimentally observed high stabilities. These two models involve two distal His conformations as reported previously for MbCNR and MbNO. However, a unique dual hydrogen bonding feature of the HNO binding was not reported before in heme protein complexes with other small molecules such as CO, NO, and O_2. These results shall facilitate investigations of HNO bindings in other heme proteins.

HNO has recently been found to play significant roles in many biological processes, such as vascular relaxation, enzyme activity regulation, and neurological function regulation.[1−4] Its pharmacological effects include enhanced cell oxidative stress, blood-brain barrier disruption, and neutrophil infiltration during renal ischemia/reperfusion.[5−7] Investigations of the HNO involvement in heme protein functions can be traced back to early studies of biological denitrification processes in plants, bacteria, and fungi by nitrite and nitric oxide reductases.[8,9] Other heme proteins, such as nitric oxide synthase, peroxidase, and cytochrome P450 nitric oxide reductase have also been suggested to include HNO as an intermediate in their catalytic cycles.[10−13] In addition, various heme proteins including metmyoglobin, methemoglobin, ferricytochrome *c*, oxymyoglobin, myoglobin, cytochrome P450, and horseradish peroxidase were used to scavenge HNO.[1]

However, to our best knowledge, no X-ray crystal structures have been reported for any HNO protein complexes and structural details of the HNO heme protein complexes at the atomic level are largely unknown. Recently, the first stable HNO heme protein complex, MbHNO (Mb, myoglobin) was isolated[14,15] and characterized by NMR, resonance Raman, and X-ray absorption spectroscopic techniques.[16,17] The NMR chemical shifts and NO vibrational frequency were found to be sensitive probes of heme active sites and bonding environments of HNO/NO^- metal complexes.[9,18−20] More recently, a novel isomer (here called MbHNO-B) was reported to coexist with the previously discovered isomer MbHNO-A, on the basis of NMR observations.[21] These results provide useful information to derive the first HNO-heme protein structural models. In fact, two MbHNO models have already been proposed based on the analysis of NMR results and force field calculation.[16,21] However, as discussed below, the prior models are unable to help understand many experimental results, which promoted us to evaluate various possibilities of MbHNO structural models using rigorous quantum chemical calculations, experimental NMR and Raman data, related protein crystallographic information, and experimental stability and reaction results. There is a growing body of work using combined X-ray, NMR, and computational studies to investigate protein active sites.[22−25] The used methods were established previously, which well reproduced both geometric and spectroscopic properties in a number of HNO and RNO (R = alkyl and aryl) metal complexes;[26] see details in the Supporting Information.

In the first structural model proposed for MbHNO-A,[16] HNO binds with the iron center via the N atom and there is one hydrogen bond (HB) with the distal His residue, which, however, was recognized to account for only partial stabilization effect for HNO binding in Mb. This is because HNO binding in Mb was experimentally observed to be much more stable than that for O_2,[9] which is isoelectronic to HNO and also has the same distal His HB. Interestingly, as shown in Table 1, a substantial error of 56 ppm in ^{15}N NMR chemical shift prediction for **1** Fe(porphyrin)(His)(HNO···His) clearly indicates another deficiency of this model. It should be noted that, in this model, the O atom in HNO forms the HB with the proton attached to the N_ε atom in the distal His group. The alternative HB model **2**, in which the H atom in HNO has the HB with the N_ε atom (thus the distal His is N_δ protonated), was also examined. As seen from Table 1, this difference only induces ≤0.1% changes in some key bond lengths and 2.8% change in ∠Fe−N−O. However, the three characteristic spectroscopic properties (NO vibrational frequency, ν_{NO}; ^1H NMR chemical shift in HNO, δ_H; ^{15}N NMR chemical shift in HNO, δ_N) show relatively larger changes, in particular δ_N changes by 9.9%. These results show that they are sensitive structural probes, which may be used to assess different structural models. Overall, results of **2** show better agreement with experimental measurements of MbHNO-A, which suggests that the

Received: May 3, 2011
Published: August 11, 2011

Table 1. Structural, Vibrational, and NMR Properties of MbHNO and Models

	system		R_{NO} (Å)	R_{NH} (Å)	R_{FeN} (Å)	∠Fe−N−O (deg)	ν_{NO} (cm^{-1})	δ_H (ppm)	δ_N (ppm)
	MbHNO-A	expt[a]	1.241		1.820	131.0	1385	14.93	661
	MbHNO-B							14.87	
1	Fe(porphyrin)(His)(HNO···His)	calcd	1.254	1.038	1.799	133.5	1374	14.88	605
2	Fe(porphyrin)(His)(His···HNO)	calcd	1.247	1.048	1.810	129.7	1400	15.55	665
3	Fe(porphyrin)(His)(H_2O···HNO···His)	calcd	1.252	1.042	1.804	131.5	1384	15.03	649
4	Fe(porphyrin)(His)(His···HNO···H_2O)	calcd	1.253	1.048	1.803	130.8	1380	15.10	664
1′	Fe(porphyrin)(His)(HNO···His)	calcd	1.250	1.039	1.802	132.6	1384	14.97	606
2′	Fe(porphyrin)(His)(His···HNO)	calcd	1.247	1.049	1.807	130.4	1401	15.63	668
3′	Fe(porphyrin)(His)(H_2O···HNO···His)	calcd	1.251	1.042	1.806	130.6	1388	15.16	649
4′	Fe(porphyrin)(His)(His···HNO···H_2O)	calcd	1.252	1.049	1.802	131.2	1382	15.16	666
1″	Fe(porphyrin)(His)(HNO···His)	calcd	1.253	1.038	1.798	133.3	1377	14.93	605
2″	Fe(porphyrin)(His)(His···HNO)	calcd	1.246	1.047	1.812	129.7	1402	15.55	659
3″	Fe(porphyrin)(His)(H_2O···HNO···His)	calcd	1.253	1.041	1.802	131.5	1380	15.04	647
4″	Fe(porphyrin)(His)(His···HNO···H_2O)	calcd	1.251	1.047	1.807	130.6	1384	15.13	658
5	Fe(protoporphyrin IX)(HNO···His)	calcd	1.255	1.038	1.797	133.9	1370	15.23	603
6	Fe(protoporphyrin IX)(HNO···His)-flip	calcd	1.254	1.038	1.797	133.6	1371	15.35	605
7	Fe(protoporphyrin IX)(H_2O···HNO···His)	calcd	1.255	1.041	1.802	131.9	1374	15.38	650
8	Fe(protoporphyrin IX)(His···HNO···H_2O)	calcd	1.254	1.047	1.803	130.7	1373	15.50	665
9	Fe(2,4-dimethyldeuteroporphyrin)(HNO···His)	calcd	1.256	1.037	1.796	133.9	1367	15.09	604
10	Fe(2,4-dimethyldeuteroporphyrin)(HNO···His)-flip	calcd	1.256	1.038	1.795	133.5	1364	15.37	605
11	Fe(2,4-dimethyldeuteroporphyrin)-(H_2O···HNO···His)	calcd	1.255	1.041	1.801	131.8	1374	15.19	645
12	Fe(2,4-dimethyldeuteroporphyrin)-(His···HNO···H_2O)	calcd	1.255	1.046	1.801	130.7	1370	15.40	662

[a] Refs 17, 18, and 21.

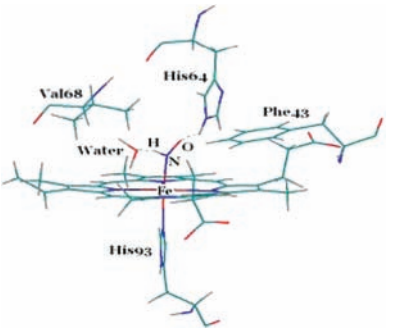

Figure 1. Illustration of MbHNO active site from using the PDB file 1DWR for MbCO with CO replaced by HNO and a water molecule. Hydrogen bonds with HNO are highlighted as the dashed lines.

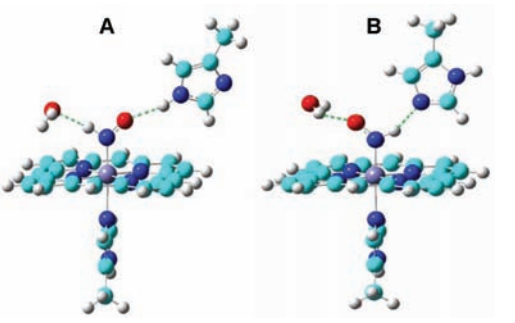

Figure 2. MbHNO active site models **3** (A) and **4** (B). Color schemes: C, cyan; O, red; N, blue; Fe, light blue; H, gray. Hydrogen bonds with HNO are highlighted as the dashed green lines.

HB model with the N_δ protonated His residue might be a better choice for isomer MbHNO-A. However, the errors of the predicted ν_{NO} and δ_H values are slightly larger than the standard deviations in the calculations.[26] Moreover, this model again has only one HB, which may not provide sufficient stabilization to support the experimentally observed high stability for MbHNO, compared to MbO_2. In fact, compared to the calculated HB energy of MbO_2,[27] the HB energies in **1** and **2** are even smaller by 3.75 and 4.43 kcal/mol, respectively.

So, what could offer the additional stabilization effect? Previous work on HNO dimer and synthetic HNO metal complex[28,29] show that HNO can be simultaneously involved in two hydrogen bonds via the terminal H and O atoms. Our prior investigations using the water molecule as a HB probe also indicate that the dual HB model is capable of supplying additional stabilization force for HNO binding[26] and provides qualitatively the best improvement in spectroscopic property predictions compared to either of the two mono HB models. However, as illustrated in Figure 1, in the Mb active site, except for the distal His residue, no other nearby residues have side chains that could form the HB with HNO. Nevertheless, there is a space for a water molecule and water is known to be viable in proteins. As a matter of fact, the active site water molecule has been found to play significant roles in some heme protein

Table 2. Statistical Results for MbHNO-A

	χ^2	Z		χ^2	Z		χ^2	Z
1	3.397	0.037	**1′**	2.799	0.061	**1″**	3.159	0.045
2	1.415	0.225	**2′**	1.703	0.161	**2″**	1.667	0.184
3	0.149	0.856	**3′**	0.235	0.769	**3″**	0.299	0.750
4	0.147	0.864	**4′**	0.125	0.858	**4″**	0.062	0.916

functions.[30,31] Therefore, a HB set of distal His and water for HNO was investigated in this work.

Because of the dissymmetry between His and water, there are in principle two kinds of dual HB models, **3** and **4**, consistent with the experimental observation of two MbHNO isomers. Interestingly, as shown in Figure 2, these two models involve two different HNO rotational conformations. They also involve two different distal His conformations (i.e., N_ε and N_δ protonated), which have been reported previously in the X-ray crystallographic and vibrational spectroscopic investigations of a number of MbCNR systems[32,33] and in the experimental and computational studies of ferric/ferrous myoglobin-NO complexes.[34,35] It should be noted that the specific dual HB model **4** is the first one that enables excellent quantitative agreement with three experimental characteristic spectroscopic properties for MbHNO-A; see Table 1. The slightly upfield experimental ^{1}H NMR shift of MbHNO-B compared to MbHNO-A[21] was also reproduced, as seen from the results of **3** versus **4**. The ^{15}N NMR shift in MbHNO-B is again predicted to be upfield than that in MbHNO-A, which is also consistent with the unpublished experimental result (Patrick J. Farmer, personal communication). Upon examination of the geometric parameters shown in Table 1, the most significant difference between **3** and **4** is in the NH bond length, which is 0.006 Å, compared to the 0.001 Å differences in NO as well as FeN bond lengths. These results suggest that the NH bond is more contracted in MbHNO-B than that in MbHNO-A, which may result in relatively higher electron densities around H and N atoms in MbHNO-B and consequently larger shielding or smaller shift as observed experimentally for MbHNO-B.

To more rigorously evaluate the four basic HNO binding motifs in **1**-**4**, a reduced χ^2 analysis and Bayesian probability (or Z-surface) technique[36] were employed. The calculations were done for MbHNO-A, since it has three experimental spectroscopic measurements. All of the three properties (ν_{NO}, δ_H, δ_N) were included in the statistical analyses (see the Supporting Information for computational details). A small χ^2 value indicates small deviation from the experiments, and a large Z value means high probability. As shown in Table 2, both types of statistical analyses consistently show that the dual HB models are of much smaller errors and much higher probabilities than the mono HB models, with **4** being the best model for MbHNO-A, in accordance with our above conclusions.

In addition, the energetic properties also support the above conclusions. The calculated HB energies in **3** and **4** show additional 8.30−9.00 kcal/mol stabilization forces compared to the respective mono HB models **1** and **2**. These effects lead to ca. 4−5 kcal/mol stronger binding forces for **3** and **4** than that in MbO_2, consistent with the observed higher stability of MbHNO over MbO_2.[9] Interestingly, experimental studies show that even photolysis or heating could not remove the second isomer that coexists with the original isomer,[21] indicating that both isomers are of similarly high stability. This is in good accordance with the above energy results. Therefore, both spectroscopic and stability results here show that, among the four basic models, **4** and **3** are the best ones for MbHNO-A and MbHNO-B, respectively.

To further examine these HNO binding motifs in Mb, two additional sets of quantum chemical geometry optimizations were done with different scopes of terminal groups of protein residues fixed at the X-ray crystal structure positions of a similar heme protein system MbCO (the same as used before in generating the first MbHNO model[16]) to mimic the protein environment effect. In contrast with the above fully optimized models **1**-**4**, the protein residues' terminal $C_\beta H_3$ groups are fixed in **1′**−**4′**. As shown in Table 1, results are similar to those from using **1**−**4**. In fact, the maximum differences of the predicted spectroscopic properties in **1′**−**4′** with respect to **1**−**4** are all within a small range of 0.4−0.9%. Compared to the data of **1**−**4** and **1′**−**4′** with protein residues truncated at C_β positions, results from using the C_α truncated **1″**−**4″** with their terminal $C_\alpha H_3$ groups fixed at X-ray geometries are also similar; see Table 1. These results support the basic HNO binding features obtained from using **1**−**4**. Nevertheless, the statistical data shown in Table 2 indicate that the quantitative agreement with MbHNO-A experiments follow the trend of **4″** > **4′** > **4**, consistent with the fact that **4** has no consideration of protein environment effect, **4′** includes this effect up to C_β places, and **4″** contains the largest scope of this effect (up to C_α positions) in these three models. Overall, statistical analyses of all these models show that the dual HB models are much better than the mono HB models, with the His···HNO···H_2O motif in **4**, **4′**, **4″** being consistently the best in each series of the models for MbHNO-A.

Besides the dual HB models, another hypothesis was proposed earlier for the two MbHNO isomers. It was suggested that the new isomer has its heme ring flipped compared to MbHNO-A, due to the use of the reconstituted protein.[21] Previous studies show that the heme orientational disorder due to protein reconstitution decays with respect to time and the final spectra become the same as with the native proteins of only one heme conformation.[37] However, for MbHNO, similar changes were not reported. In fact, even with photolysis or heating the two isomers still coexist. Moreover, reaction details suggest that the synthesis of the new isomer is correlated with the way of generating HNO, rather than the heme orientation due to protein reconstitution.[21] For instance, even though the reconstituted proteins were used in both syntheses, MbHNO-B was prepared only from using $NaNO_2/NaBH_4$, while only MbHNO-A was reported from using a more mild reducing agent $Na_2S_2O_4$ compared to $NaBH_4$. In addition, for the same reconstituted protein that contains the new isomer, the reactions of first oxidizing it, then reducing it to Fe^{II}Mb, and finally reintroducing HNO with the old method (not the new $NaNO_2/NaBH_4$ method) resulted in only the old isomer, MbHNO-A.

To computationally investigate the heme ring flipping effect, protoporphyrin IX was used, for which the heme peripheral substituents were kept except that the propionate terminal CO_2^- group is modified to CH_3. Results of using the first proposed MbHNO-A model, Fe(protoporphyrin IX)(HNO···His) **5**, and its heme ring flipped one Fe(protoporphyrin IX)(HNO···His)-flip **6**, as well as the two dual HB models **7** and **8** are shown in Table 1. The predicted small difference in the δ_H values between **5** and **6** is similar to the experimental ring flipping effect reported previously for MbCO.[37] However, as exemplified by the substantial errors in the predicted ^{15}N NMR chemical shifts for **5** and **6**, together with their less stable mono HB features for HNO, these two models are unlikely to be the actual MbHNO

structures. Overall, the maximum differences between results of using protoporphyrin IX models and corresponding nonsubstituted porphyrins are all less than 1% for both geometric and spectroscopic properties, except for the δ_H change, which is ca. 2%. The experimental trend of upfield NMR chemical shifts in MbHNO-B than MbHNO-A is retained in the dual HB models **7** and **8**. Clearly, these comparisons support the conclusions from using nonsubstituted porphyrin models. Additional calculations using the 2,4-dimethyldeuteroporphyrin models (**9**−**12**) for corresponding reconstituted myoglobin complexes again show similar results (see the Supporting Information for more details).

Overall, this work led to the discovery of the first atomic level MbHNO structural models that are in excellent agreement with numerous experimental spectroscopic and stability results. Several sets of quantum chemical calculations and statistical analyses support the binding motif of His···HNO···H_2O for MbHNO-A and H_2O···HNO···His for MbHNO-B, involving two different HNO rotational conformers. The statistical data for MbHNO-A show that among **4**, **4′**, **4″** with the same correct binding motif, the more inclusion of protein environment effect, the better quantitative agreement with experiments, that is, **4″** > **4′** > **4**. These models also indicate an important role of the distal His conformation in priming substrate bindings, as reported previously for MbCNR and MbNO systems.[32−35] In addition, they also highlight the role of the active site water molecule as found with other heme proteins.[30,31] The heme ring flipping effect was found to yield small NMR shift differences as observed experimentally in a similar heme protein system,[37] but this effect is unlikely to account for the reported two MbHNO isomers due to inconsistence with some experimental spectroscopic, stability, and reaction results. It is interesting to note that the dual HB feature is unique for HNO binding in Mb, compared to the bindings of other small molecules such as CO, NO, and O_2. These results shall facilitate investigations of HNO interactions with other heme proteins.

■ ASSOCIATED CONTENT

Supporting Information. Computational details and other information (Figure S1 and Tables S1−S20). This material is available free of charge via the Internet at http://pubs.acs.org.

■ AUTHOR INFORMATION

Corresponding Author
yong.zhang@stevens.edu

■ ACKNOWLEDGMENT

This work was supported by the NIH Grant GM-085774. Y.Z. thanks Patrick J. Farmer for sharing experimental NMR results of the MbHNO isomers before publication and Eric Oldfield for helpful discussion.

■ REFERENCES

(1) Miranda, K. M. *Coord. Chem. Rev.* **2005**, *249*, 433–455.
(2) Nagasawa, H. T.; Demaster, E. G.; Redfern, B.; Shirota, F. N.; Goon, J. W. *J. Med. Chem.* **1990**, *33*, 3120–3122.
(3) Sidorkina, O.; Espey, M. G.; Miranda, K. M.; Wink, D. A.; Laval, J. *Free Radical Biol. Med.* **2003**, *35*, 1431–1438.
(4) Shinyashiki, M.; Chiang, K. T.; Switzer, C. H.; Gralla, E. B.; Valentine, J. S.; Thiele, D. J.; Fukuto, J. M. *Proc. Natl. Acad. Sci. U.S.A.* **2000**, *97*, 2491–2496.
(5) Boje, K. M. K.; Lakhman, S. S. *J. Pharmacol. Exp. Ther.* **2000**, *293*, 545–550.
(6) Booth, B. P.; Tabrizi-Fard, M. A.; Fung, H. L. *Biochem. Pharmacol.* **2000**, *59*, 1603–1609.
(7) Nagasawa, H. T.; Demaster, E. G.; Redfern, B.; Shirota, F. N.; Goon, J. W. *J. Med. Chem.* **1990**, *33*, 3120–3122.
(8) Averill, B. A. *Chem. Rev.* **1996**, *96*, 2951–2964.
(9) Farmer, P. J.; Sulc, F. *J. Inorg. Biochem.* **2005**, *99*, 166–184.
(10) Rusche, K. M.; Spiering, M. M.; Marletta, M. A. *Biochemistry* **1998**, *37*, 15503–15512.
(11) Huang, J. M.; Sommers, E. M.; Kim-Shapiro, D. B.; King, S. B. *J. Am. Chem. Soc.* **2002**, *124*, 3473–3480.
(12) Miranda, K. M.; Paolocci, N.; Katori, T.; Thomas, D. D.; Ford, E.; Bartberger, M. D.; Espey, M. G.; Kass, D. A.; Feelisch, M.; Fukuto, J. M.; Wink, D. A. *Proc. Natl. Acad. Sci. U.S.A.* **2003**, *100*, 9196–9201.
(13) Lehnert, N.; Praneeth, V. K. K.; Paulat, F. *J. Comput. Chem.* **2006**, *27*, 1338–1351.
(14) Lin, R.; Farmer, P. J. *J. Am. Chem. Soc.* **2000**, *122*, 2393–2394.
(15) Sulc, F.; Immoos, C. E.; Pervitsky, D.; Farmer, P. J. *J. Am. Chem. Soc.* **2004**, *126*, 1096–1101.
(16) Sulc, F.; Fleischer, E.; Farmer, P. J.; Ma, D. J.; La Mar, G. N. *J. Biol. Inorg. Chem.* **2003**, *8*, 348–352.
(17) Immoos, C. E.; Sulc, F.; Farmer, P. J.; Czarnecki, K.; Bocian, D. F.; Levina, A.; Aitken, J. B.; Armstrong, R. S.; Lay, P. A. *J. Am. Chem. Soc.* **2005**, *127*, 814–815.
(18) Kumar, M. R.; Pervitsky, D.; Chen, L.; Poulos, T.; Kundu, S.; Hargrove, M. S.; Rivera, E. J.; Diaz, A.; Colon, J. L.; Farmer, P. J. *Biochemistry* **2009**, *48*, 5018–5025.
(19) Montenegro, A. C.; Amorebieta, V. T.; Slep, L. D.; Martin, D. F.; Roncaroli, F.; Murgida, D. H.; Bari, S. E.; Olabe, J. A. *Angew. Chem., Int. Ed.* **2009**, *48*, 4213–4216.
(20) Pellegrino, J.; Bari, S. E.; Bikiel, D. E.; Doctorovich, F. *J. Am. Chem. Soc.* **2010**, *132*, 989–995.
(21) Kumar, M. R.; Fukuto, J. M.; Miranda, K. M.; Farmer, P. J. *Inorg. Chem.* **2010**, *49*, 6283–6292.
(22) Lai, J.-F.; Niks, D.; Wang, Y.-C.; Domratcheva, T.; Barends, T. R. M.; Schwarz, F.; Olsen, R. A.; Elliott, D. W. F., M. Q.; Chang, C.-E. A.; Schlichting, I.; Dunn, M. F.; Mueller, L. J. *J. Am. Chem. Soc.* **2010**, *133*, 4–7.
(23) Vulpetti, A.; Schiering, N.; Dalvit, C. *Proteins* **2010**, *78*, 3281–3291.
(24) Viegas, A.; Brás, N. F.; Cerqueira, N. M.; Fernandes, P. A.; Prates, J. A.; Fontes, C. M.; Bruix, M.; Romão, M. J.; Carvalho, A. L.; Ramos, M. J.; Macedo, A. L.; Cabrita, E. J. *FEBS J.* **2008**, *275*, 2524–2535.
(25) Mao, J. H.; Mukherjee, S.; Zhang, Y.; Cao, R.; Sanders, J. M.; Song, Y. C.; Zhang, Y. H.; Meints, G. A.; Gao, Y. G.; Mukkamala, D.; Hudock, M. P.; Oldfield, E. *J. Am. Chem. Soc.* **2006**, *128*, 14485–14497.
(26) Ling, Y.; Mills, C.; Weber, R.; Yang, L.; Zhang, Y. *J. Am. Chem. Soc.* **2010**, *132*, 1583–1591.
(27) Ling, Y.; Zhang, Y. In *Annual Reports in Computational Chemistry*; Wheeler, R. A., Ed.; Elsevier: New York, 2010; Vol. 6, pp 65−77.
(28) Liu, Y.; Liu, W. Q.; Li, H. Y.; Liu, J. G.; Yang, Y. *J. Phys. Chem. A* **2006**, *110*, 11760–11764.
(29) Sellmann, D.; Gottschalk-Gaudig, T.; Haussinger, D.; Heinemann, F. W.; Hess, B. A. *Chem.—Eur. J.* **2001**, *7*, 2099–2103.
(30) Derat, E.; Shaik, S.; Rovira, C.; Vidossich, P.; Alfonso-Prieto, M. *J. Am. Chem. Soc.* **2007**, *129*, 6346–6347.
(31) Lai, W.; Chen, H.; Shaik, S. *J. Phys. Chem. B* **2009**, *113*, 7912–7917.
(32) Smith, R. D.; Blouin, G. C.; Johnson, K. A.; Phillips, G. N.; Olson, J. S. *Biochemistry* **2010**, *49*, 4977–4986.
(33) Blouin, G. C.; Olson, J. S. *Biochemistry* **2010**, *49*, 4968–4976.
(34) Miller, L. M.; Pedraza, A. J.; Chance, M. R. *Biochemistry* **1997**, *36*, 12199–12207.
(35) Soldatova, A. V.; Ibrahim, M.; Olson, J. S.; Czernuszewicz, R. S.; Spiro, T. G. *J. Am. Chem. Soc.* **2010**, *132*, 4614–4625.
(36) Zhang, Y.; Gossman, W.; Oldfield, E. *J. Am. Chem. Soc.* **2003**, *125*, 16387–16396.
(37) Jue, T.; Krishnamoorthi, R.; La Mar, G. N. *J. Am. Chem. Soc.* **1983**, *105*, 5701–5703.